Quality & Quantity (2025) 59:5769–5793
https://doi.org/10.1007/s11135-025-02235-2

Valuing advertising investment with modular strategies under copula-based dependence

Lucianna Cananà[1] · Guglielmo D'Amico[2] · Salvatore Vergine[3]

Accepted: 2 June 2025 / Published online: 23 June 2025

Abstract

In this work, we estimate the value of a contract between a company seeking to advertise its business on two or more television channels and a television network. Specifically, we present a method for evaluating a real option that allows advertisements to be broadcast on multiple channels while considering the dependence structure of the dynamics of viewers among the different channels by a copula function. We model the dynamics of viewers through a Markov reward process, and we use a specific function to transform it into earnings. Then, we compute the n-th-order moment of the total discounted payoffs to find the probability distribution of the payoff function and price the option. Finally, we propose an empirical application using real television audience data, introducing the hypothesis of modular strategies. Specifically, we assume that the advertisements are broadcast at selected times depending on the channel. For simplicity of study, we consider the case of two channels, but the proposed methodology can be immediately extended to more channels.

Keywords Markov chain · Real Option approach · Copula functions · Advertising

These authors contributed equally to this work.

✉ Salvatore Vergine
s.vergine@staff.univpm.it

Lucianna Cananà
lucianna.canana@uniba.it

Guglielmo D'Amico
g.damico@unich.it

1 Ionic Department in Legal and Economic Systems of the Mediterranean: Society, Environment, Culture, University of Bari Aldo Moro, Piazza Umberto I, 70121 Taranto, Italy

2 Department of Economics, University G. d'Annunzio of Chieti–Pescara, Viale Pindaro, 42, 65127 Pescara, Italy

3 Department of Management, Marche Polytechnic University, Piazzale R. Martelli, 8, 60121 Ancona, Italy

1 Introduction

Mass media have been a crucial instrument for marketers to engage consumers and advertise their products. Of all available media, television advertising has remained the dominant choice for reaching large audiences with a global investment in TV and video advertising of more than 300 billion USD in 2023 (Arslan et al 2024).

The advertising industry attempts to drive and influence public attitudes and behaviors about the information aired (O'Keefe and Reid 2020) and represents a significant source of exposure to advertising for all types of audiences (Pauze and Potvin Kent 2021; Krishnamurthi and Raj 1985; Pechmann and Catlin 2016). Most sectors are influenced by the advertising industry that attempts to shape consumer behavior, such as tobacco and alcohol-related advertising (Davis 2008) or food and nutrition advertising (Pechmann and Catlin 2016).

In addition, advertising expenditure is characterized by a long-term positive impact on the market capitalization of its own firms (Joshi and Hanssens 2010). Various scientific studies and meta-analyses on advertising effectiveness have been published, which highlight the challenges in measuring advertising effectiveness. In this regard, the work in Oetzel and Luppold (2024) suggests methods for estimating the return on marketing investment to optimize budget allocation.

In this context, quantifying advertising costs is fundamental to rule the relationship arising between the company that wants to offer its advertising campaign and the company that owns and/or manages the television network. These costs refer to information, reputation, and other intangible services provided by regularly implemented advertising campaigns (Martin-Oliver and Salas-Fumas 2008). The authors in Danaher and Rust (1996) consider advertising an investment and find the optimal expenditure to maximize the return without giving importance to timing and placement (channel). On the other hand, Tellis et al (2005) evaluate the effect of TV advertising on sales by separating the effects of advertising itself from those of other factors, such as time, placement and age of the market. In particular, they propose a two-stage hierarchical design model to estimate the effectiveness of both various ads across markets and of the ads as a function of the measured ad creative characteristics, i.e., emotion and argument.

A method to assess advertising costs is provided by the real options (RO) approach. It has been widely used in the literature and is suitable for valuing the contract between companies (Lo and Lan 2010; Di Bari et al 2024; Cucchiella and Gastaldi 2006). Different price methods can be identified, such as the Black and Scholes (B&S) option pricing model, Binomial Option Pricing Model (BOPM), and the Monte Carlo method (Black and Scholes 1973; Cox et al 1979; Di Bari et al 2024; Abdel Sabour and Poulin 2006).

In this regard, a relevant contribution is provided by D'Amico et al (2024) that aims at estimating the value of a contract between a television network and a company willing to advertise its business on this network. The authors propose a real option approach in which the company advertising its business has the possibility to exercise the option at a future time to choose between airing the advertisement or not, in exchange for a price paid today. The price of the option depends on the probability density function of the sum of discounted cash flows, generated according to a Markov reward process, where the dynamics of viewers is the main random variable and directly influences the payoff. The proposed framework has at least two important limitations that need to be overcome. The first one consists of considering only a channel on which the advertisement can be aired. This choice is clearly motivated by reasons of simplicity and should be removed as the allocation of advertising budget between multiple channels is a common strategy to support sales in multiple markets (see, e.g., Abedi (2017)). The second weakness of the model considered in D'Amico et al (2024) stems from the adoption of a regular timetable when the advertisement should be transmitted. In particular, the authors fix a set of times, during which the advertisement is on the air. Nonetheless, it can be of interest relaxing this assumption and assessing the effect of a strategy that determines whether the channel can broadcast advertising at that time or not. The removal of these limitations is the main objective of this study and passes for the adoption of a more general mathematical model that allows increasing flexibility, efficiency and ensures that the model is well adapted in the best possible manner to the actual reality.

Hence, this work advances the research presented in D'Amico et al (2024) by proposing a novel methodology capable of considering multiple channels together with a modular strategy that allows advertising to be broadcast at different times for each channel. The modularity refers to the ability to choose both the channels and time slots for broadcasting the advertisement. This modular structure offers greater flexibility and adaptability to new information, which is particularly valuable in dynamic and uncertain environments such as TV advertising. The proposed methodology addresses the problem in its full generality by incorporating these new aspects.

The possibility of airing an advertising campaign on multiple platforms simultaneously could introduce challenges related to audience dependence, as viewers may choose to follow one channel or platform over another. This creates a dependency issue in audience dynamics, where the viewership of one medium may influence or be influenced by the viewership of another, making it essential to accurately model these inter-dependencies. To this end, copula-based models represent a very versatile and extensively applied tool to model the dependence structure. They have found large applications in many fields of study, such as marketing analysis (Gabriel et al 2024; Goodwin et al 2024), financial analysis (Cherubini et al 2004; Durante et al 2015), power system uncertainty analysis (Papaefthymiou and Kurowicka 2008; D'Amico et al 2015), as well as in Markovian framework (Hu et al 2017; D'Amico et al 2020, 2019).

Furthermore, we develop recurrent type equations for the moments of the discounted accumulated reward process, which expresses the total gain arising from the advertisement policy. This is done by considering the adopted modulated strategy of advertising as a new element of the theory and we recover the classical approach when the policy consists of airing the advertisement at every time of the regular scheduled timetable. Therefore, the obtained results are relevant not only to the specific problem of advertisement evaluation but also more in general for the theory of Markov reward processes. Finally, we use the obtained moments to calculate the density function of the television advertisement through the maximum entropy approach defined by Mead and Papanicolaou (1984), and compute the option price.

At the end of the work, we present an application of the proposed methodology in which we use audience data from an Italian television network downloaded from Auditel (2024). In particular, these data have a monthly discretization and provide eight time slots for each month. We apply the proposed model to two television channels, Canale 5 and Italia 1, which are part of the Mediaset network. The transition probability matrix obtained using a Markov process effectively captures the dynamics of the audience over time. Additionally, we employ the Farlie-Gumbel-Morgenstern (FGM) copula to account for cash flow dependence between the multiple channels. Finally, we analyze two distinct advertising scheduling scenarios: one with synchronized advertisements and the other with unsynchronized placements. The obtained results demonstrate greater accuracy when higher-order moments are used, compared to the classical B&S model, which relies only on two moments. Therefore, the results validate the mathematical model presented in this study.

The remainder of the paper comprises Sect. 2 where the model for the option pricing and the moments computation are presented together with the recursive algorithm used to obtain the solution of formulas. In Sect. 3, we present the data used to apply the model and the results obtained for the case study proposed. Finally, Sect. 4 concludes this work and discusses possible extensions and further research.

2 Methodology

We now present the model used to price the option and the computation of the k-th moment of the total discount cash flows generated from airing the advertisements on different channels. Furthermore, we also introduce the recursive algorithm to compute the moments.

2.1 Model for option pricing

Let A be a company that plans to launch its advertising campaign to a television network, denoted as company B. We assume that the latter owns two different channels, but the methodology and results are directly scalable to a more complex framework.

The two companies may agree on airing the advertisement in correspondence with a selection of times belonging to the vector of time $t_1^n = (t_1, t_2, ..., t_n)$. This possibility needs to be formalized mathematically. Hence, we consider a function $\pi : \mathbb{R}^n \rightarrow \mathbb{R}$, $\pi = \pi(t_1^n)$ such that $\forall i = 1, 2, ..., n,\ t_i = t_i(h, l)$ with $h, l \in \{0, 1\}$, with the convention that

- $h = 0$ means no advertising is broadcast on the first channel;
- $h = 1$ means advertising is broadcast on the first channel;
- $l = 0$ means no advertising is broadcast on the second channel;
- $l = 1$ means advertising is broadcast on the second channel.

To give an example, $\pi = \pi\big(t_1(1,0), t_2(1,1), t_3(0,1)\big)$ means that at time t_1 the advertising is broadcast only on the first channel, at time t_2 on both channels and at time t_3 only on the second channel.

The two companies sign an option contract that grants the company A the opportunity to advertise its business on the television network of company B in exchange for paying a premium. We suppose that at time $t = 0$ the option has the price P and it can be exercised at the strike price K at time t_0, which is the time to maturity of the option. Exercising the option gives to the company A the right to air multiple advertisements at future times $t_1, ..., t_n$ according to the strategy $\pi(t_1^n)$.

We consider the fixed discount rate, r, and we compute the sum of all the discounted cash flows, i.e., the stochastic discounted cash flows, as

$$Z_\pi = \sum_{i=1}^{n} e^{-(t_i - t_0)r} \left(\hat{G}^{(1)}(t_i) + \hat{G}^{(2)}(t_i) \right) = \sum_{i=1}^{n} e^{-(t_i - t_0)r} \hat{G}^{EMPTY}(t_i), \tag{1}$$

with

$$\hat{G}^{(1)}(t_i) = G^{(1)}(t_i) \cdot 1_{\{h_i = 1\}}, \quad \hat{G}^{(2)}(t_i) = G^{(2)}(t_i) \cdot 1_{\{l_i = 1\}},$$

and

$$\hat{G}(t_i) = \hat{G}^{(1)}(t_i) + \hat{G}^{(2)}(t_i).$$

$\hat{G}^{(1)}(t_i)$ and $\hat{G}^{(2)}(t_i)$ are the cash flows generated by channels 1 and 2, respectively, in the case in which the advertising is broadcast at time t_i. Indeed, G represents the potential earnings, which turn into actual earnings $\hat{G}$ if the advertisement is broadcast at the considered time. The cash flow is shown in Fig. 1 where the times t_i are not necessarily equispaced.

Then, we consider a European call option and we define the payoff function as

$$W = \max(Z - K, 0).$$

Finally, we have all the elements to compute the option price as

$$\mathbb{E}[W] = \int_K^\infty z \cdot f_Z(z)dz,$$

where f_Z is the density function of the random variable Z. The exact knowledge of this density function is obtained using the same approach applied in D'Amico et al (2024), where the author first compute the moments of the Z process and, then, use the maximum entropy approach defined by Mead and Papanicolaou (1984) to recover the density function.

The computation of the higher-order moments requires the adoption of specific assumptions. The first hypothesis, as done in D'Amico et al (2024), considers the number of viewers behaving like a Markov chain. The random variable $\{J_n\}_{n\in\mathbb{N}}$ indicates the regime of the viewers and has a finite state space $E = \{1, 2, ..., s\}$. Therefore, we have s states, each representing a different level of audience. The chain respects the following Markov property:

$$\begin{aligned}\mathbb{P}(J_{i+1} = j_{i+1} | J_i = j_i, J_{i-1} = j_{i-1}, ..., J_0 = j_0) &= \mathbb{P}(J_{i+1} = j_{i+1} | J_i = j_i) \\ &= p_{j_i j_{i+1}}\end{aligned}$$

where $p_{j_i j_{i+1}}$ represents the probability to reach state j_{i+1} starting from state j_i in one period. The probabilities are stored in the transition probability matrix $\mathbf{P} = (p_{ij})_{i,j\in E}$.

Then, we consider a second assumption concerning the structure of the cash flows generated by broadcasting advertisements on channel a at time t_m, denoted by $G^{(a)}(t_m)$. Specifically, we assume that the cash flows obtained by company B from advertising on channel a depend solely on the current regime $J_{t_m} = i_m$. This means that, for every time $\forall\, t_m \in \mathbb{N}$ and

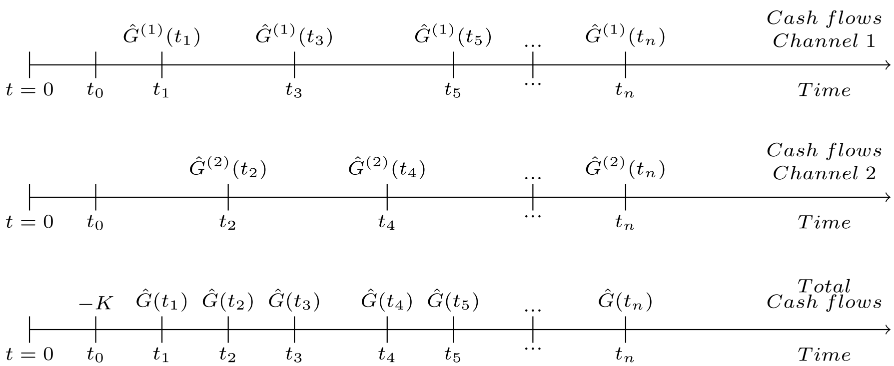

Fig. 1 Cash flow of the option.

channel $\forall\, a \in \{1,2\}$, the distribution of $G^{(a)}(t_m)$ is independent of the specific time, of any past payoffs, and of past regimes. This is mathematically expressed as follows:

$$\mathcal{D}\big(G^{(a)}(t_m)|J_{t_m} = i_m, J_{t_{m-1}} = i_{m-1}, ..., J_{t_0} = i_0, G^{(a)}(t_{m-1}) = x_{m-1}, ..., G^{(a)}(t_0) = x_0\big)$$
$$= \mathcal{D}\big(G^{(a)}(t_m)|J_{t_m} = i_m\big) =: F^{(a)}_{i_m},$$

where, in general, $\mathcal{D}\big(X\big)$ denotes the probability distribution of the random variable X.

We assume that $F^{(a)}_{i_m}$ is absolutely continuous and, therefore, admits density $f^{(a)}_{i_m}$. We also hypothesize that there is dependence between contemporary payoffs of the two channels, that is

$$\mathcal{D}\big(G^{(1)}(t_m), G^{(2)}(t_m)|J_{t_m} = i_m\big) = C_\theta(F^{(1)}_{i_m}, F^{(2)}_{i_m}), \tag{2}$$

where $C_\theta(F^{(1)}_{i_m}, F^{(2)}_{i_m})$ is a parametric copula with marginal distribution functions $F^{(1)}_{i_m}$ and $F^{(2)}_{i_m}$ of channels 1 and 2 and parameter θ.

Remark 1 If we relax the previous assumptions by considering independence between the cash flows of the two channels, set one of them to zero, and further considering a non-modular strategy, we obtain the same results as those in (D'Amico et al 2024).

Given the complexity introduced by the assumptions of modular strategy and dependence structure of the audience of multiple channels, the computation of the k moments is particularly challenging. To address this, we derive the moments recursively, as shown in the next two subsections.

2.2 Moments computation

We proceed to the calculation of the k-th moment of Z conditioned to the starting state $J_{t_0} = j_0$. We refer to the vector t^n_0 of components $(t_0, t_1, ..., t_n)$ indicating the vectors of times the advertisements are aired. We also consider two additional vectors h^n_1 and l^n_1 with values in $\{0,1\}^n$ and define $t_1 = t_1(h_i, l_i)$ $\forall i = 1, ..., n$. Furthermore, the chosen strategy is $\pi = \pi(t^n_1) = \pi\big((t\big(h^n_1, l^n_1\big)\big) = \Big(\pi\big((t\big(h_1, l_1\big)\big), \pi\big((t\big(h_2, l_2\big)\big), ..., \pi\big((t\big(h_n, l_n\big)\big)\Big)$ establishing when the advertisements are aired on the two channels. We have that

$$
\begin{aligned}
M_{j_0}^{(k)}\left(t_0^n;\pi\left(t(h_1^n,l_1^n)\right)\right) &:= \mathbb{E}\left[(Z_\pi)^k|J_0=j_0\right]\\
&= \mathbb{E}\left[\sum_{i=1}^{n} e^{-r(t_i-t_0)}\left(G^{(1)}(t_i)1_{\{h_i=1\}}+G^{(2)}(t_i)1_{\{l_i=1\}}\right)^k\middle|J_{t_0}=j_0\right]\\
&= \mathbb{E}\Bigg[e^{-r(t_1-t_0)}\left(G^{(1)}(t_i)1_{\{h_i=1\}}+G^{(2)}(t_i)1_{\{l_i=1\}}\right)\\
&+\sum_{a=2}^{n} e^{-r(t_a-t_0)}\left(G^{(1)}(t_a)1_{\{h_a=1\}}+G^{(2)}(t_a)1_{\{l_a=1\}}\right)^k\Bigg|J_{t_0}=j_0\Bigg]\\
&= \sum_{s=0}^{k}\binom{k}{s}\mathbb{E}\Bigg[\left(e^{-r(t_1-t_0)}G^{(1)}(t_1)1_{\{h_1=1\}}+G^{(2)}(t_1)1_{\{l_1=1\}}\right)^s\\
&\left(\sum_{a=2}^{n} e^{-r(t_a-t_0)}\left(G^{(1)}(t_a)1_{\{h_a=1\}}+G^{(2)}(t_a)1_{\{l_a=1\}}\right)\right)^{k-s}\Bigg|J_{t_0}=j_0\Bigg]\\
&= \mathbb{E}\left[\left(e^{-r(t_1-t_0)}\left(G^{(1)}(t_i)1_{\{h_i=1\}}+G^{(2)}(t_i)1_{\{l_i=1\}}\right)\right)^k\middle|J_{t_0}=j_0\right]\\
&+\sum_{s=1}^{k-1}\binom{k}{s}\mathbb{E}\Bigg[\left(e^{-r(t_1-t_0)}G^{(1)}(t_1)1_{\{h_1=1\}}+G^{(2)}(t_1)1_{\{l_1=1\}}\right)^s\\
&\cdot\left(\sum_{a=2}^{n} e^{-r(t_a-t_0)}\left(G^{(1)}(t_a)1_{\{h_a=1\}}+G^{(2)}(t_a)1_{\{l_a=1\}}\right)\right)^{k-s}\Bigg|J_{t_0}=j_0\Bigg]\\
&+\mathbb{E}\left[\left(\sum_{a=2}^{n} e^{-r(t_a-t_0)}\left(G^{(1)}(t_a)1_{\{h_a=1\}}+G^{(2)}(t_a)1_{\{l_a=1\}}\right)\right)^k\middle|J_{t_0}=j_0\right]
\end{aligned} \tag{3}
$$

Subsequently, we can proceed by computing the three expected values obtained in the equation (3). The first one is :

$$
\begin{aligned}
&\mathbb{E}\left[\left(e^{-r(t_1-t_0)}\left(G^{(1)}(t_i)1_{\{h_i=1\}}+G^{(2)}(t_i)1_{\{l_i=1\}}\right)\right)^k\middle|J_{t_0}=j_0\right]\\
&=\mathbb{E}\left[\mathbb{E}\left[\left(e^{-r(t_1-t_0)}\left(G^{(1)}(t_i)1_{\{h_i=1\}}+G^{(2)}(t_i)1_{\{l_i=1\}}\right)\right)^k\middle|J_{t_1},J_{t_0}=j_0\right]\middle|J_{t_0}=j_0\right].
\end{aligned}
$$

By first considering the internal expected value, we have that

$$
\begin{aligned}
&\mathbb{E}\left[\left(e^{-r(t_1-t_0)}\left(G^{(1)}(t_i)1_{\{h_i=1\}}+G^{(2)}(t_i)1_{\{l_i=1\}}\right)\right)^k\middle|J_{t_1},J_{t_0}=j_0\right]\\
&= e^{-r(t_1-t_0)k}\int_0^{+\infty}\int_0^{+\infty}(x_1 1_{\{h_1=1\}}+x_2 1_{\{l_1=1\}})^k f_{J_{t_1}}(x_1,x_2)dx_1dx_2
\end{aligned}
$$

Consequently, we obtain

$$
\begin{aligned}
&\mathbb{E}\left[\mathbb{E}\left[\left(e^{-r(t_1-t_0)}\left(G^{(1)}(t_i)1_{\{h_i=1\}}+G^{(2)}(t_i)1_{\{l_i=1\}}\right)\right)^k\middle|J_{t_1},J_{t_0}=j_0\right]\middle|J_{t_0}=j_0\right]\\
&=\sum_{j_1\in E} p_{j_0,j_1}^{(t_1-t_0)}\left(e^{-r(t_1-t_0)k}\int_0^{+\infty}\int_0^{+\infty}(x_1 1_{\{h_1=1\}}+x_2 1_{\{l_1=1\}})^k f_{j_1}(x_1,x_2)dx_1dx_2\right)
\end{aligned}
$$

The quantity $p_{j_0,j_1}^{(t_1-t_0)}$ is the probability of reaching the state j_1 at the time t_1 starting from the state j_0 at the time t_0, obtainable as the place element j_0,j_1 of the t_1-t_0 power of transition matrix $\mathbf{P}$, i.e., $p_{j_0,j_1}^{(t_1-t_0)} = \left(\mathbf{P}^{(t_1-t_0)}\right)_{j_0,j_1}$.

As follows, we calculate the second expected value using the tower property of the conditional expectation operator. We have that

$$\begin{aligned}
&\sum_{s=1}^{k-1}\binom{k}{s}\mathbb{E}\Bigg[\left(e^{-r(t_1-t_0)}G^{(1)}(t_1)1_{\{h_1=1\}}+G^{(2)}(t_1)1_{\{l_1=1\}}\right)^s \\
&\quad\cdot\left(\sum_{a=2}^{n}e^{-r(t_a-t_0)}\left(G^{(1)}(t_a)1_{\{h_a=1\}}+G^{(2)}(t_a)1_{\{l_a=1\}}\right)\right)^{k-s}\Bigg|J_{t_0}=j_0\Bigg] \\
&=\mathbb{E}\Bigg[\mathbb{E}\Big[\left(e^{-r(t_1-t_0)}G^{(1)}(t_1)1_{\{h_1=1\}}+G^{(2)}(t_1)1_{\{l_1=1\}}\right)^s \\
&\quad\cdot\left(\sum_{a=2}^{n}e^{-r(t_a-t_0)}\left(G^{(1)}(t_a))1_{\{h_a=1\}}+G^{(2)}(t_a)1_{\{l_a=1\}}\right)\right)^{k-s} \\
&\quad\Big|J_{t_1},G^{(1)}(t_1),G^{(2)}(t_1),J_{t_0}=j_0\Big]\Bigg|J_{t_0}=j_0\Bigg]
\end{aligned}\tag{4}$$

We observe that the random variable $e^{-r(t_1-t_0)}G^{(1)}(t_1)1_{\{h_1=1\}}+G^{(2)}(t_1)1^s_{\{l_1=1\}}$ is $\left(J_{t_1},G^{(1)}(t_1),G^{(2)}(t_1)\right)$ measurable and, therefore, can exit from the internal expected value of the equation (4). Indeed, we have that

$$\begin{aligned}
&\mathbb{E}\Bigg[\mathbb{E}\Big[\left(e^{-r(t_1-t_0)}G^{(1)}(t_1)1_{\{h_1=1\}}+G^{(2)}(t_1)1_{\{l_1=1\}}\right)^s \\
&\quad\cdot\left(\sum_{a=2}^{n}e^{-r(t_a-t_0)}\left(G^{(1)}(t_a))1_{\{h_a=1\}}+G^{(2)}(t_a)1_{\{l_a=1\}}\right)\right)^{k-s} \\
&\quad\Big|J_{t_1},G^{(1)}(t_1),G^{(2)}(t_1),J_{t_0}=j_0\Big]\Bigg|J_{t_0}=j_0\Bigg] \\
&=\mathbb{E}\Bigg[\left(e^{-r(t_1-t_0)}G^{(1)}(t_1)1_{\{h_1=1\}}+G^{(2)}(t_1)1_{\{l_1=1\}}\right)^s \\
&\quad\cdot\Big[\mathbb{E}\left(\sum_{a=2}^{n}e^{-r(t_a-t_0)}\left(G^{(1)}(t_a))1_{\{h_a=1\}}+G^{(2)}(t_a)1_{\{l_a=1\}}\right)\right)^{k-s} \\
&\quad\Big|J_{t_1},G^{(1)}(t_1),G^{(2)}(t_1)\Big]\Bigg|J_{t_0}=j_0\Bigg].
\end{aligned}$$

We now consider the internal expected value, as follows.

$$\mathbb{E}\left[\left(\sum_{a=2}^{n} e^{-r(t_a-t_0)}\big(G^{(1)}(t_a))1_{\{h_a=1\}} + G^{(2)}(t_a)1_{\{l_a=1\}}\big)\right)^{k-s}\middle| J_{t_1}, G^{(1)}(t_1), G^{(2)}(t_1)\right]$$
$$= e^{-r(t_1-t_0)(k-s)}\mathbb{E}$$
$$\left[\left(\sum_{a=2}^{n} e^{-r(t_a-t_0)}\big(G^{(1)}(t_a))1_{\{h_a=1\}} + G^{(2)}(t_a)1_{\{l_a=1\}}\big)\right)^{k-s}\middle| J_{t_1}, G^{(1)}(t_1), G^{(2)}(t_1)\right]$$
$$= e^{-r(t_1-t_0)(k-s)}M^{(k-s)}_{J_{t_1}}\left(t_1^n;\pi\big(t(h_2^n, l_2^n)\big)\right).$$

Then, we obtain the second expected value.

$$\sum_{s=1}^{k-1}\binom{k}{s}\mathbb{E}\Bigg[\big(e^{-r(t_1-t_0)}G^{(1)}(t_1)1_{\{h_1=1\}} + G^{(2)}(t_1)1_{\{l_1=1\}}\big)^{s}$$
$$\cdot\left(\sum_{a=2}^{n} e^{-r(t_a-t_0)}\big(G^{(1)}(t_a)1_{\{h_a=1\}} + G^{(2)}(t_a)1_{\{l_a=1\}}\big)\right)^{k-s}\Bigg| J_{t_0} = j_0\Bigg]$$
$$= \sum_{j_1\in E} p^{(t_1-t_0)}_{j_0 j_1}\Bigg[e^{-r(t_1-t_0)s}\int_0^{+\infty}\int_0^{+\infty}(x_1 1_{\{h_1=1\}} + x_2 1_{\{l_1=1\}})^s f_{j_1}(x_1,x_2)dx_1dx_2$$
$$\cdot e^{-r(t_1-t_0)(k-s)}M^{(k-s)}_{J_1}\left(t_1^n;\pi\big(t(h_2^n, l_2^n)\big)\right)\Bigg]$$
$$= \sum_{j_1\in E} p^{(t_1-t_0)}_{j_0 j_1}e^{-r(t_1-t_0)k}\Bigg[\int_0^{+\infty}\int_0^{+\infty}(x_1 1_{\{h_1=1\}} + x_2 1_{\{l_1=1\}})^s f_{j_1}(x_1,x_2)dx_1dx_2$$
$$M^{(k-s)}_{j_1}\left(t_1^n;\pi\big(t(h_2^n, l_2^n)\big)\right)\Bigg].$$

Finally, we calculate the third expected value, as follows:

$$\mathbb{E}\left[\left(\sum_{a=2}^{n} e^{-r(t_a-t_0)}\big(G^{(1)}(t_a)1_{\{h_a=1\}} + G^{(2)}(t_a)1_{\{l_a=1\}}\big)\right)^{k}\middle| J_{t_0} = j_0\right]$$
$$= \mathbb{E}\left[\mathbb{E}\left[\left(\sum_{a=2}^{n} e^{-r(t_a-t_0)}\big(G^{(1)}(t_a)1_{\{h_a=1\}} + G^{(2)}(t_a)1_{\{l_a=1\}}\big)\right)^{k}\middle| J_{t_1}, J_{t_0} = j_0\right]\middle| J_{t_0} = j_0\right]$$
$$= \sum_{j_1\in E} p^{(t_1-t_0)}_{j_0 j_1}\left[e^{-r(t_1-t_0)k}M^{(k)}_{j_1}\left(t_1^n;\pi\big(t(h_2^n, l_2^n)\big)\right)\right]$$

Now we have all the elements to obtain the main result of this study. We compute the k-th moment of Z conditioned to the starting state $J_{t_0} = j_0$ of our process, as follows:

$$M_{j_0}^{(k)}(t_0^n;\pi(h_1^n,l_1^n)) = \sum_{J_1\in E} p_{j_0,j_1}^{(t_1-t_0)} e^{-r(t_1-t_0)k}$$
$$\Bigg[\int_0^{+\infty}\int_0^{+\infty}(x_1 1_{\{h_1=1\}}+x_2 1_{\{l_1=1\}})^k f_{j_1}(x_1,x_2)dx_1dx_2$$
$$+\sum_{s=1}^{k-1}\binom{k}{s}\int_0^{+\infty}\int_0^{+\infty}(x_1 1_{\{h_1=1\}}+x_2 1_{\{l_1=1\}})^s f_{j_1}(x_1,x_2)dx_1dx_2$$
$$M_{j_1}^{(k-s)}\left(t_1^n;\pi\left(t(h_2^n,l_2^n)\right)\right)+M_{j_1}^{(k)}\left(t_1^n;\pi\left(t(h_2^n,l_2^n)\right)\right)\Bigg]. \quad (5)$$

The calculations carried out up to this point are valid for any specification of the joint density. However, according to the assumption expressed in formula (2), the density takes the following form:

$$f_j(x_1,x_2) = c\left(F_j^{(1)},F_j^{(2)}\right)f_j(x_1)f_j(x_2), \quad \forall j\in E,$$

where

$$c(u,v) = \frac{\theta^2 c(u,v)}{\theta u\theta v}$$

is the density of the copula.

Thus, the recursive equation that expresses the k-th order moment is as follows:

$$M_{j_0}^{(k)}(t_0^n;\pi(h_1^n,l_1^n)) = \sum_{J_1\in E} p_{j_0,j_1}^{(t_1-t_0)} e^{-r(t_1-t_0)k}$$
$$\cdot\Bigg[\int_0^{+\infty}\int_0^{+\infty}(x_1 1_{\{h_1=1\}}+x_2 1_{\{l_1=1\}})^k c\left(F_{j_1}^{(1)},F_{j_1}^{(2)}\right)f_{j_1}(x_1)f_{j_1}(x_2)dx_1dx_2$$
$$+\sum_{s=1}^{k-1}\binom{k}{s}\int_0^{+\infty}\int_0^{+\infty}(x_1 1_{\{h_1=1\}}+x_2 1_{\{l_1=1\}})^s c\left(F_{j_1}^{(1)},F_{j_1}^{(2)}\right)f_{j_1}(x_1)f_{j_1}(x_2)dx_1dx_2$$
$$M_{j_1}^{(k-s)}\left(t_1^n;\pi\left(t(h_2^n,l_2^n)\right)\right)+M_{j_1}^{(k)}\left(t_1^n;\pi\left(t(h_2^n,l_2^n)\right)\right)\Bigg]. \quad (6)$$

The equation exhibits a recursive structure with respect to the vector of times t_0^n as well as the order of the moments. It is interesting to note that, for specific values of the parameter θ, we can obtain the moments under the assumption of independence between earnings from the two channels. Moreover, the appropriately defined strategy π allows us to determine the marginal earnings for individual channels, as well as to visualize the modularity effects of the strategy.

2.3 Recursive algorithm

We present the algorithm applied for the computation of the moments. It consists of the following steps:

1. First of all, we set $k = 1$ to obtain

$$M_{j_0}^{(1)}\left(t_0^n;\pi\left(t(h_1^n,l_1^n)\right)\right) = \sum_{j_1\in E} p_{j_0,j_1}^{(t_1-t_0)} e^{-r(t_1-t_0)}\Bigg[\int_0^{+\infty}\int_0^{+\infty}(x_1 1_{\{h_1=1\}}+x_2 1_{\{l_1=1\}}) f_{j_1}(x_1,x_2)dx_1dx_2 + M_{j_1}^{(1)}\left(t_1^n;\pi\left(t(h_2^n,l_2^n)\right)\right)\Bigg].$$

2. Then, to solve the previous equation, we set $t_0 = t_{n-1}$, which is equivalent to $t_1 = t_n$. Thus, we obtain

$$M_{j_{n-1}}^{(1)}\left(t_{n-1}^n;\pi\left(t(h_n^n,l_n^n)\right)\right) = \sum_{j_n\in E} p_{j_{n-1},j_n}^{(t_n-t_{n-1})} e^{-r(t_n-t_{n-1})}\Bigg[\int_0^{+\infty}\int_0^{+\infty}(x_1 1_{\{h_n=1\}}+x_2 1_{\{l_n=1\}}) f_{j_n}(x_1,x_2)dx_1dx_2 + M_{j_n}^{(1)}\left(t_n^n;\pi\left(t(h_{n+1}^n,l_{n+1}^n)\right)\right)\Bigg].$$

We observe that $M_{j_n}^{(1)}\left(t_n^n;\pi\left(t(h_{n+1}^n,l_{n+1}^n)\right)\right)$ is null by definition $\forall\pi$. We therefore have that

$$M_{j_{n-1}}^{(1)}\left(t_{n-1}^n;\pi\left(t(h_n^n,l_n^n)\right)\right) = \sum_{j_n\in E} p_{j_{n-1},j_n}^{(t_n-t_{n-1})} e^{-r(t_n-t_{n-1})} \cdot\left[\int_0^{+\infty}\int_0^{+\infty}(x_1 1_{\{h_n=1\}}+x_2 1_{\{l_n=1\}}) f_{j_n}(x_1,x_2)dx_1dx_2\right]. \tag{7}$$

We can observe that all the terms on the right of the equation (7) are known terms.

3. Following this, we set $t_0 = t_{n-2}$, which is identical to saying $t_1 = t_{n-1}$, to find the following solution:

$$M_{j_{n-2}}^{(1)}\left(t_{n-2}^n;\pi\left(t(h_{n-1}^n,l_{n-1}^n)\right)\right) = \sum_{j_{n-1}\in E} p_{j_{n-2},j_{n-1}}^{(t_{n-1}-t_{n-2})} e^{-r(t_{n-1}-t_{n-2})} \cdot\Bigg[\int_0^{+\infty}\int_0^{+\infty}(x_1 1_{\{h_{n-1}=1\}}+x_2 1_{\{l_{n-1}=1\}}) \cdot f_{j_{n-1}}(x_1,x_2)dx_1dx_2 + M_{j_{n-1}}^{(1)}\left(t_{n-1}^n;\pi\left(t(h_n^n,l_n^n)\right)\right)\Bigg]. \tag{8}$$

We note that $M_{j_{n-1}}^{(1)}\left(t_{n-1}^n;\pi\left(t(h_n^n,l_n^n)\right)\right)$ is already calculated in formula (7). Therefore, we can solve the formula (8) given that all the terms are known. We proceed recursively by setting $t_0 = t_{n-3}$ in order to obtain $M_{j_0}^{(1)}\left(t_0^n;\pi\left(t(h_1^n,l_1^n)\right)\right)$.

4. Then, we set $k = 2$ to obtain

$$M_{j_0}^{(2)}\left(t_0^n;\pi\left(t(h_1^n,l_1^n)\right)\right) = \sum_{j_1\in E} p_{j_0,j_1}^{(t_1-t_0)} e^{-2r(t_1-t_0)}\Bigg[\int_0^{+\infty}\int_0^{+\infty}(x_1 1_{\{h_1=1\}}+x_2 1_{\{l_1=1\}}) f_{j_1}(x_1,x_2)dx_1dx_2 + 2\int_0^{+\infty}\int_0^{+\infty}(x_1 1_{\{h_1=1\}}+x_2 1_{\{l_1=1\}}) f_{j_1}(x_1,x_2)dx_1dx_2 \, M_{j_1}^{(1)}\left(t_1^n;\pi\left(t(h_2^n,l_2^n)\right)\right) + M_{j_1}^{(2)}\left(t_1^n;\pi\left(t(h_2^n,l_2^n)\right)\right)\Bigg].$$

Table 1 Statistics of AMR for the channels Canale 5 and Italia 1

Statistics	Canale 5	Italia 1
Mean	1,945,000	665,777
Median	1,844,926	544,543
Minimum	359,774	4.41
Maximum	4,756,835	4,372,852
Standard deviation	1,002,336	551,545
Fisher asymmetry index	0.61	2.47
Pearson's Kurtosis index	2.64	13.30

We observe that we obtained the term $M^{(1)}_{j_1}\left(t^n_1;\pi\left(t(h^n_2,l^n_2)\right)\right)$ through the equation (8) and, therefore we consider it as known. Then, we iterate the process by setting $t_0 = t_{n-1}$, then, $t_0 = t_{n-2}$, and so on.

5. Finally, we set $k = 2$ and $t_0 = t_{n-1}$, which corresponds to $t_1 = t_n$ and obtain that

$$M^{(2)}_{j_{n-1}}\left(t^n_{n-1};\pi\left(t(h^n_n,l^n_n)\right)\right) = \sum_{j_n\in E} p^{(t_n-t_{n-1})}_{j_{n-1}j_n} e^{-2r(t_n-t_{n-1})}\Bigg[\int_0^{+\infty}\int_0^{+\infty}(x_1 1_{\{h_n=1\}} + x_2 1_{\{l_n=1\}})^2$$
$$f_{j_n}(x_1,x_2)dx_1dx_2 + 2\int_0^{+\infty}\int_0^{+\infty}(x_1 1_{\{h_n=1\}} + x_2 1_{\{l_n=1\}})f_{j_n}(x_1,x_2)dx_1dx_2$$
$$M^{(1)}_{j_n}\left(t^n_n;\pi\left(t(h^n_{n+1},l^n_{n+1})\right)\right) + M^{(2)}_{j_n}\left(t^n_n;\pi\left(t(h^n_{n+1},l^n_{n+1})\right)\right)\Bigg].$$

We note that $M^{(1)}_{j_n}\left(t^n_n;\pi\left(t(h^n_{n+1},l^n_{n+1})\right)\right) = 0$ and $M^{(2)}_{j_n}\left(t^n_n;\pi\left(t(h^n_{n+1},l^n_{n+1})\right)\right) = 0$ and the other terms are known.

3 Case study

In this section, we present the data used to apply the model and the results obtained from applying the analysis in the following two cases: the first in which the advertising schedule is synchronized for the two channels and the second in which it is unsynchronized.

To apply the proposed model, we download audience data from Auditel (2024), referred to the Italian television network.[1] We choose two channels, namely Canale 5 and Italia 1 and collect the data from January 2017 to December 2021. More precisely, the data consists of monthly average minute rating (AMR) data giving the average number of viewers for the following eight slots: 2:00 am-7:00 am, 7:00 am-9:00 am, 9:00 am-12:00 pm, 12:00 pm-3:00 pm, 3:00 pm-6:00 pm, 6:00 pm-8:30 pm, 8:30 pm-10:30 pm and 10:30 pm-2:00 am. Thus, we have a total of 480 monthly observations for each channel. Some statistics of the AMR are shown in Table 1.

[1] Auditel is a Joint Industry Committee, an independent industry body that brings together all stakeholders in the television market. It provides audience monthly averages and minute-by-minute averages, though the latter are not freely accessible.

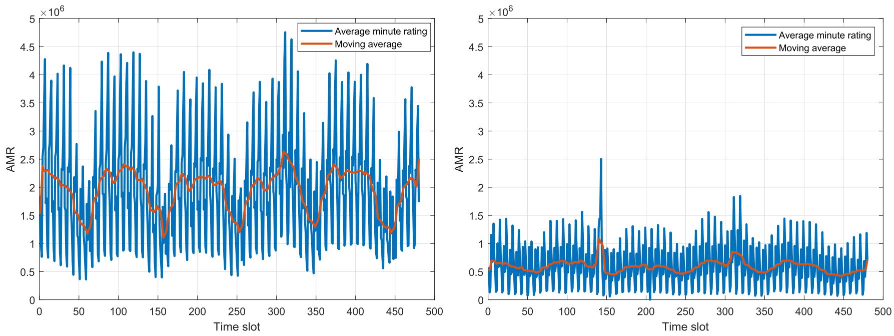

Fig. 2 Time series of AMR with the moving average for the channels “Canale 5”(**a**) and “Italia 1” (**b**).

Table 2 Statistics of the AMR moving averages for the channels Canale 5 and Italia 1

Statistics	Canale 5	Italia 1
Mean	1,944,909	592,789
Median	2,060,597	590,549
Minimum	1,099,719	422,928
Maximum	2,632,300	1,080,646
Standard deviation	358,185	100,495
Fisher asymmetry index	−0.61	1.17
Pearson’s Kurtosis index	2.26	6.40

The two channels exhibit significant differences in terms of mean, median, and standard deviation, with Canale 5 showing higher values across all three metrics. In particular, Canale 5 is characterized by a higher level of audience, reaching an average of 1,945,000, against 665,000 of Italia 1. Also, the standard deviation is almost double for Canale 5 compared to Italia 1. Furthermore, Italia 1 presents a much higher Fisher’s skewness index and Pearson’s kurtosis index, indicating a more asymmetric and heavy-tailed distribution of audience measurements.

As follows, we graph the two data series and the corresponding moving averages with a period equal to eight (corresponding to the number of time slots within each month) in Fig. 2a, b . These plots highlight the monthly and yearly seasonality characterizing the two databases.

Furthermore, Table 2 reports the descriptive statistics of the AMR moving averages for Canale 5 and Italia 1. Canale 5 exhibits a significantly higher mean audience compared to Italia 1, highlighting its broader reach and market dominance. The coefficient of variation (computed as the ratio between the standard deviation and the mean) is 18.41% for Canale 5 and 16.95%, indicating a slightly higher relative variability in the audience of Canale 5 compared to Italia 1. The Fisher asymmetry index and Pearson’s kurtosis index indicate differing distributional shapes. Canale 5 presents a slightly left-skewed distribution (−0.61), implying a longer left tail and a higher concentration of higher-than-average values. Conversely, Italia 1 is right-skewed (1.17), with a higher probability of extremely high values. Additionally, Italia 1 shows a Pearson’s Kurtosis index greater than three, suggesting a higher frequency of outliers, whereas Canale 5 has a distribution closer to normality in terms of the behavior of the tails.

Also, to visually assess the correlation structure between the moving averages of audience of the two channels, we provide a scatter plot for Canale 5 and Italia 1. As shown in Fig. 3, the two series show a linear correlation coefficient ρ =0.64, indicating a moderate to strong positive linear relationship.

To apply the proposed model, first, we sum the two series "Canale 5"and "Italia 1"to obtain a unique time series. Then, to identify the viewing regimes, we remove the periodic component by computing the moving average over a period corresponding to the number of slots available each month, which is eight. The resulting moving average, shown in Fig. 4, has a mean $\mu = 2.538 \cdot 10^6$ and a standard deviation $\sigma = 4.294 \cdot 10^5$.

We also show the histogram of the total moving average and the values of μ, $\mu - \frac{\sigma}{1.25}$, and $\mu + \frac{\sigma}{1.25}$ in Fig. 5. The frequencies of the discretized observations reaches the highest values on the left of the average μ because the distribution presents a heavy tail on the left.

We apply the Markov model to the moving average series by discretizing it according to a state space E made of s =4 states. The states are delimited by the values $\mu - \frac{\sigma}{1.25}$, μ and $\mu + \frac{\sigma}{1.25}$. Therefore, we classify the moving average values depending on whether they are smaller than or equal to $\mu - \frac{\sigma}{1.25}$ indicated by state 1, greater than $\mu - \frac{\sigma}{1.25}$ and smaller than or equal to μ indicated by state 2, greater than μ and smaller than or equal to $\mu + \frac{\sigma}{1.25}$ indicated by state 3, and greater than $\mu + \frac{\sigma}{1.25}$ indicated by state 4. We show the transition probability matrix $\mathbf{P}$ that we obtain using the maximum likelihood estimation (Billingsley 1961; Bharucha-Reid 1962), as follows:

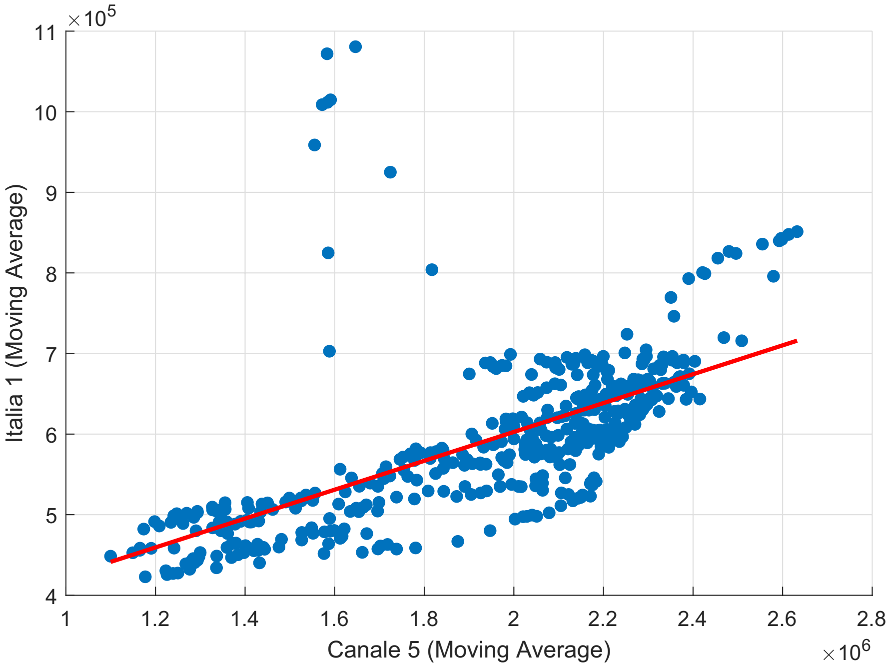

Fig. 3 Scatter plot of the AMR moving averages for Canale 5 and Italia 1 and their linear regression line.

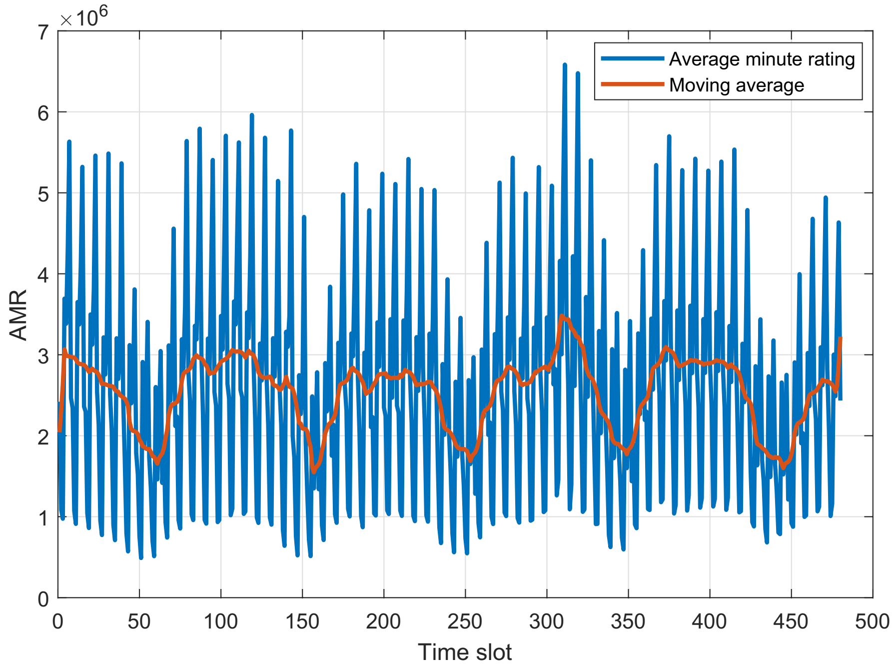

Fig. 4 Total time series of AMR with the rolling average

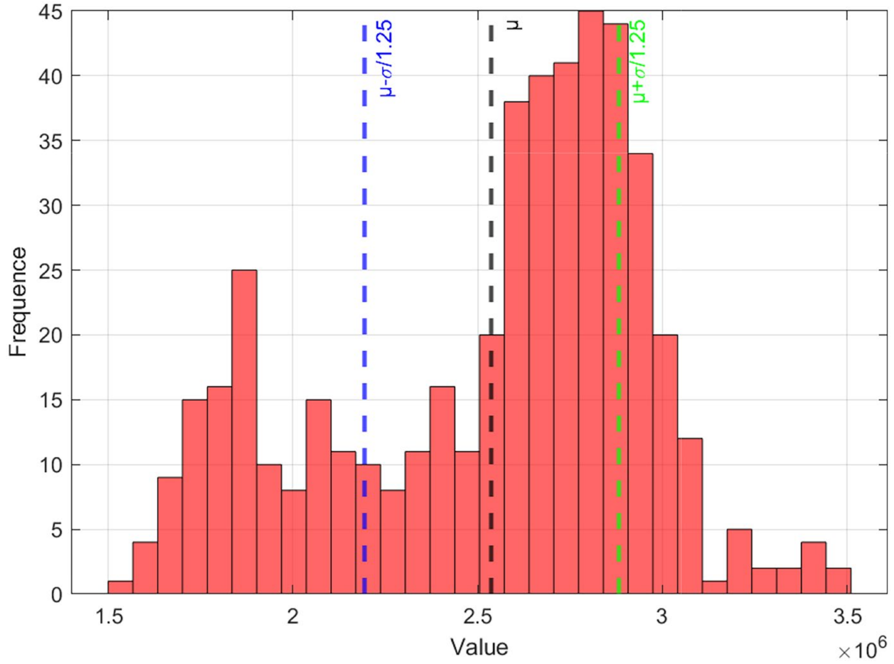

Fig. 5 Histogram of total moving average and values of μ, $\mu - \frac{\sigma}{1.25}$, and $\mu + \frac{\sigma}{1.25}$

$$\mathbf{P} = \begin{array}{c} \\ 1 \\ 2 \\ 3 \\ 4 \end{array} \begin{array}{c} \begin{array}{cccc} 1 & 2 & 3 & 4 \end{array} \\ \begin{pmatrix} 0.950 & 0.050 & 0.00 & 0.00 \\ 0.085 & 0.797 & 0.118 & 0.00 \\ 0.000 & 0.030 & 0.925 & 0.045 \\ 0.000 & 0.000 & 0.080 & 0.920 \end{pmatrix} \end{array}.$$

We notice that the matrix is diagonally dominant as the greater values are located on the main diagonal which means that the probability of remaining in the same state at the next transition is high. The corresponding stationary distribution is

$$\boldsymbol{\pi} = [0.192\ 0.113\ 0.445\ 0.250],$$

where we can see that the probabilities are spread with the highest value corresponding to state 3.

To estimate the cumulative distribution function of the gains, we assume that the cash-flow function $G(\cdot)$ consists of a linear function of the number of viewers N who watch the TV channel at each time t. We decide to follow the same choice as in D'Amico et al (2024) due to the absence of specific audience data. We introduce the function $G : \mathbb{N}_0 \to \mathbb{R}^+$ such that

$$G(N(t_i)) = N(t_i).$$

We plot the empirical cumulative distribution function (ECDF) conditionally on state 1, state 2, state 3, and state 4 for the moving average of "Canale 5", "Italia 1", and the total series in Fig. 6a–d , respectively. As we expect, the ECDF of the total series reaches higher values and it is always located on the right side of each graph.

Then, we decide to apply the Farlie-Gumbel-Morgenstern (FGM) copula (Cambanis 1977). It represents an important family of copulas and it is defined as follows:

$$C(u, v) = uv + \theta uv(1 - u)(1 - v) \qquad \text{with } -1 \le \theta \le 1,$$

where the parameter θ has the following meanings:

- $\theta = 0$ indicates independence between the variables;
- $\theta > 0$ indicates moderate positive dependence;
- $\theta < 0$ indicates moderate negative dependence.

The density of this copula is:

$$c(u, v) = 1 + \theta(1 - 2u)(1 - 2v).$$

This copula is particularly useful and frequently used for its easy estimation and implementation. Therefore, we decided to apply the FGM copula only to show the proposed methodology of application of copulas in this domain.[2] Also, given its tractability and flexibility,

[2] The choice of the best copula fitting a data set can be done according to standard estimation techniques, see, e.g., Cherubini et al (2004). However, we do not carry out this analysis in the present study due to the lack of data with sufficient granularity. This aspect is left for future research, once more detailed data become available.

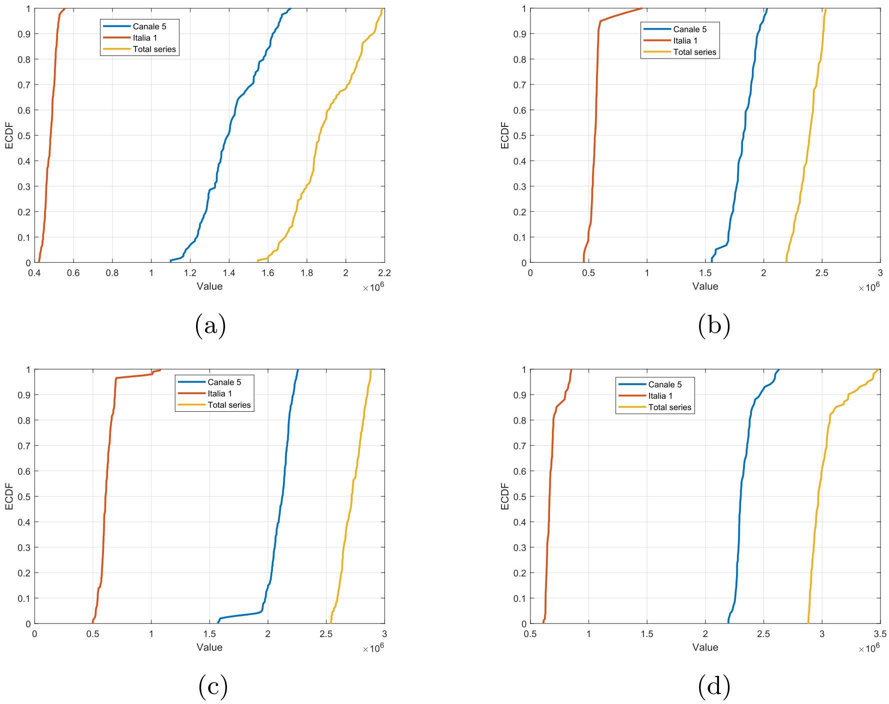

Fig. 6 Empirical Cumulative Distribution Function (ECDF) of the total series and of "Canale 5"and "Italia 1"series for state 1 (**a**), state 2 (**b**), state 3 (**c**), and state 4 (**d**)

the FGM copula provides a suitable framework for capturing the joint distribution of these variables. From the application of the FGM copula, we obtain the results in terms of the dependence parameter θ estimated using the maximum likelihood estimation (MLE) and shown in Table 3.

As is noticeable, we obtain positive dependence for states 1 and 4, meaning that the tail values of the two series show the same behaviour. Vice versa, the two series show a negative dependence for the central values identified with states 2 and 3. These characteristics are also visible in Fig. 7, where we graph the joint density function for each state. We can notice that when the dependence parameter θ is positive (state 1 and state 4), the shape of the function highlights a positive association of the two series, indicating that as the audience on Canale 5 increases, the audience on Italia 1 also increases, and vice versa. In contrast, when the dependence parameter θ is negative, the shape of the function reflects an inverse relationship between the two series, which indicates a negative association. Therefore, when the audience regime is in state 2 or 3, the two channels are in competition, meaning that an increase in viewership on one channel tends to correspond to a decrease on the other.

Table 3 Values of θ for each state

State	1	2	3	4
θ	1.0000	−0.4456	−0.0147	1.0000

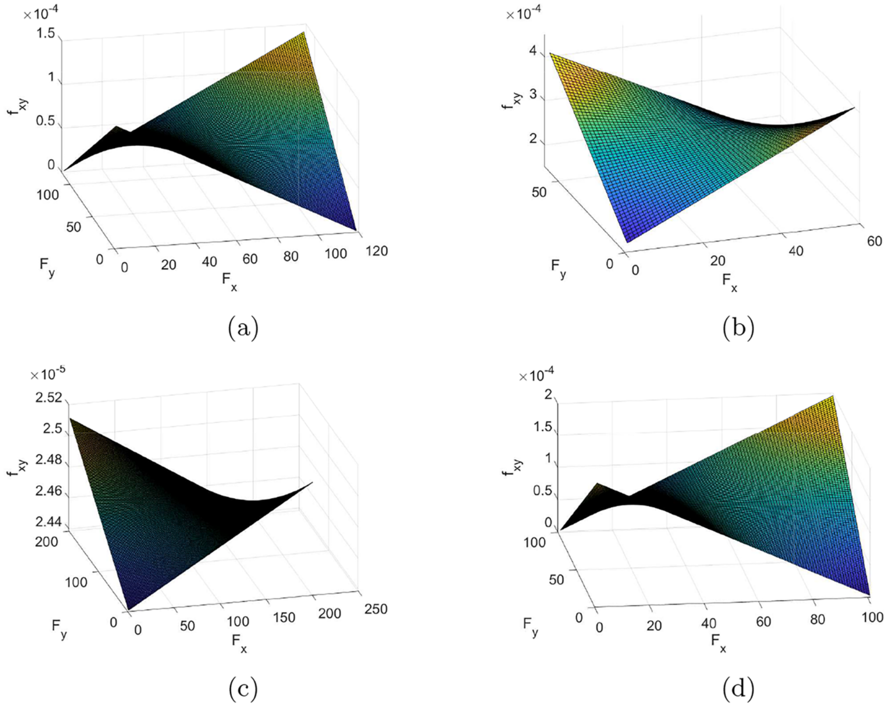

Fig. 7 Estimated Joint Density Function of the Empirical Copula for state 1 (**a**), state 2 (**b**), state 3 (**c**), and state 4 (**d**)

3.1 Analysis of Synchronized Advertising Scheduling

We hypothesize that the two channels air the advertisement at the same time and we set the time vector equal to $\mathbf{t}_0^3 = [4, 12, 16, 20]$. The strategy considered in this application is

$$\pi = \pi\big(t_1(1,1), t_2(1,1), t_3(1,1)\big). \tag{9}$$

Then, we apply formula (1) to compute the sum of all the discounted cash flows at the current time t_0, conditionally to the regime $J_0 = 1$. This means that the regime indicated by the Markov process is the lowest at the initial time $t = 0$. We can obtain the first- and second-order moments through formula (6). The expected value of the total discounted cash flows amounts to $1.477 \cdot 10^6$ for Canale 5, with a standard deviation of $2.093 \cdot 10^5$. The expected value and the standard deviation for Italia 1 are $4.921 \cdot 10^5$ and $4.562 \cdot 10^4$, respectively. We observe that Canale 5 shows a significantly higher mean value compared to Italia 1, indicating that its expected revenue is substantially greater. The standard deviation values suggest that the variability in discounted cash flows is also higher for Canale 5, implying greater fluctuations in financial performance across simulations.

Table 4 First six moments in millions conditioning at each of the four states for the time vector $\mathbf{t}_0^3$ and strategy $\pi = \pi\left(t_1(1,1), t_2(1,1), t_3(1,1)\right)$.

k	$J_0 = 1$	$J_0 = 2$	$J_0 = 3$	$J_0 = 4$
1	1.488	1.764	1.994	2.117
2	2.269	3.193	4.013	4.510
3	3.548	5.917	8.141	9.659
4	5.704	11.191	16.639	20.788
5	9.436	21.545	34.239	44.953
6	16.075	42.125	70.916	97.638

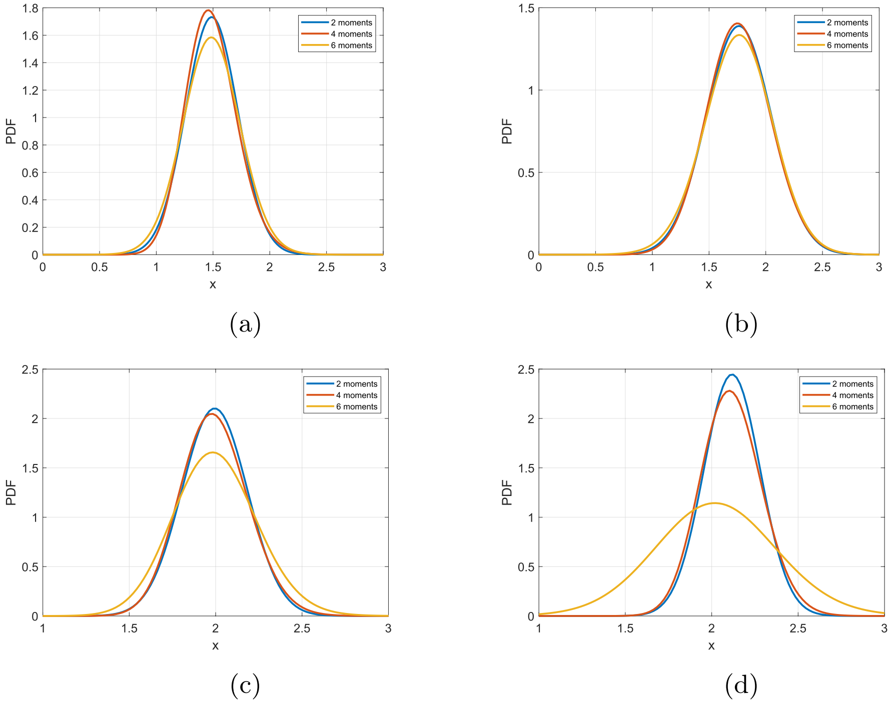

Fig. 8 Density functions starting from the knowledge of 2, 4, and 6 moments conditioning on state 1 (a), state 2 (b), state 3 (c), and state 4 (d) for $\mathbf{t}_0^3$ and strategy $\pi = \pi\left(t_1(1,1), t_2(1,1), t_3(1,1)\right)$.

At this point, we can compute the first six moments conditioning at each state using Eq. (5).[3] The obtained results in millions are shown in Table 4.

As it is noticeable, the results exhibit monotonic increasing trends both in the moment order k and in the initial state J_0. This fact indicates that higher-order moments capture progressively larger deviations from the mean, especially for greater initial states. These monotonic trends in moment estimates are fundamental for constructing the probability density function using the maximum entropy approach.

[3] We use the discount rate r =3.533% taken equal to the 12-month Italian Treasury Bonds rate of the 10th April 2024 published by the Italian Ministry of Economy and Finance.

Table 5 Option prices in euros for different values of strike price K conditioning at each state and employing the density function obtained by considering the first six moments for $\mathbf{t}_0^3$ and strategy $\pi = \pi\big(t_1(1,1), t_2(1,1), t_3(1,1)\big)$

K	$J_0 = 1$	$J_0 = 2$	$J_0 = 3$	$J_0 = 4$
1,500,000	804,658	1,525,883	1,971,654	1,931,629
2,000,000	67,673	412,024	1,055,279	1,179,737
2,500,000	4,075	15,161	64,368	233,076
3,000,000	3,568	3,338	5,323	11,777

Table 6 Option prices in euros for different values of strike price K conditioning at each state and employing the density function obtained by considering the lognormal distribution for $\mathbf{t}_0^3$ and strategy $\pi = \pi\big(t_1(1,1), t_2(1,1), t_3(1,1)\big)$

K	$J_0 = 1$	$J_0 = 2$	$J_0 = 3$	$J_0 = 4$
1,500,000	797,001	1,234,246	1,800,270	1,844,963
2,000,000	51,532	390,112	947,422	977,353
2,500,000	3,825	11,856	43,866	287,248
3,000,000	3,427	4,036	5,566	9,299

Fig. 8a–d show the density functions obtained from the knowledge of two, four, and six moments conditioning on state 1, 2, 3, and 4, respectively.

It can be seen that the higher the states, the heavier the tails of the distribution, and therefore, the more we need higher-order moments. For example, the six-order moment distribution shows heavy tails indicating that extreme events are significantly more likely and, therefore the probability of having very low and very high viewership regions of the two channels is high.

We employ the density function obtained by considering the first six moments to compute the option price. We show the obtained results in Table 5.

The monotonic trend is generally preserved across the states, except for the strike price of 1,500,000 in the fourth distribution ($J_0 = 4$). This exception occurs because the distribution at $J_0 = 4$ has a heavy tail also on the left side, affecting the pricing behaviour at lower strike prices.

To ensure the robustness of our model, we validate our findings by comparing them with results derived from a parametric lognormal distribution, which is consistent with the framework of the Black-Scholes model. We consider a random variable $X = e^N$ that follows the lognormal distribution $logX(\mu, \sigma^2)$ when $N = logX$ follows the normal distribution $N(\mu, \sigma^2)$. Subsequently, we consider the following probability density function:

$$f(x) = \frac{e^{-\frac{(lnx-\mu)^2}{2\sigma^2}}}{x\sqrt{2\pi\sigma}},$$

with $\mathbb{E}[\mathbb{X}] = \mathbb{e}^{+\frac{2}{2}}$ and $Var(X) = e^{2\mu+\sigma^2}(e^{\sigma^2} - 1)$.

Following this approach, we obtain the results in Table 6.

The values in Tables 5 and 6 show a similar trend with a decrease in the option price when the strike price K increases, and an increase when the status increases. Furthermore, we can notice that the B&S model exhibits an underpricing of the option due to its lognormality assumption, which is not observed in real data. Our model is non-parametric and allows for option pricing that aligns more closely with empirical data.

3.2 Analysis of unsynchronized advertising scheduling

In this scenario, the advertising times for the two channels are not synchronized but differ slightly. In particular, we set $\mathbf{t}_0^6 = [4, 12, 13, 16, 17, 20, 21]$ and fix the strategy

$$\pi = \pi\big(t_1(1,0), t_2(0,1), t_3(1,0), t_4(0,1), t_5(1,0), t_6(0,1)\big). \tag{10}$$

This strategy no longer involves broadcasting the advertisement simultaneously on both channels but instead schedules it to air first on Canale 5 and then on Italia 1 at the next time. This variation in timing can provide insights into how staggered advertising slots may influence audience overlap and the effectiveness of each campaign. Also, in this case, we compute the first six moments conditioned at each state. The obtained results in millions are shown in Table 7.

The results continue to exhibit monotonic increasing trends both in the moment order k and in the initial state J_0 but are generally lower than the ones obtained for the synchronized advertising case. This fact indicates that unsynchronized scheduling reduces the concentration of viewership, leading to lower overall audience engagement. This suggests that staggering advertisements across different time slots may dilute peak audience responses, potentially affecting the effectiveness of the campaigns.

As follows, we apply the maximum entropy approach and we show the density functions obtained from the knowledge of two, four, and six-moment conditioning on states 1, 2, 3, and 4 in Fig. 9a–d , respectively.

We notice that the behaviour remains stable with the six-order moment distributions showing heavy tails for starting states $J_0 = 3$ and $J_0 = 4$, although they are more contained compared to the synchronized advertising case.

As follows, we compute the option price by considering the first six moments and we show the results in Table 8.

The monotonic trend is generally maintained across the states, with higher initial states (J_0) leading to higher option prices. However, compared to the synchronized advertising case, the option prices are lower overall. This suggests that the staggered advertising schedule results in a lower expected payoff, likely due to reduced audience overlap and, consequently, lower expected revenues. Additionally, at higher strike prices, the option values converge across different states, indicating a diminishing impact of the initial state as the strike price increases.

Also, in this case, we show the results of the robustness test proposed in the previous subsection in Table 9.

Table 7 First six moments in millions conditioning at each of the four states for $\mathbf{t}_0^6$ and strategy $\pi = \pi\big(t_1(1,0), t_2(0,1), t_3(1,0), t_4(0,1), t_5(1,0), t_6(0,1)\big)$.

k	$J_0 = 1$	$J_0 = 2$	$J_0 = 3$	$J_0 = 4$
1	1.141	1.354	1.546	1.643
2	1.339	1.894	2.414	2.715
3	1.621	2.723	3.801	4.508
4	2.022	4.005	6.029	7.522
5	2.601	6.004	9.624	12.608
6	3.445	9.141	15.451	21.224

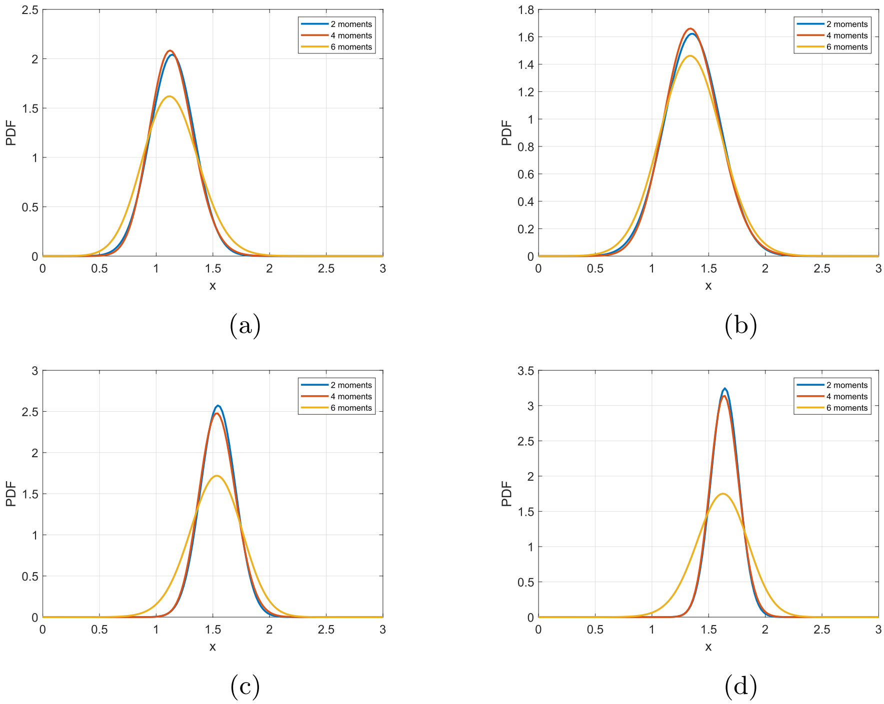

Fig. 9 Density functions starting from the knowledge of 2, 4, and 6 moments conditioning on state 1 (a), state 2 (b), state 3 (c), and state 4 (d) for $\mathbf{t}_0^6$ and strategy $\pi = \pi\left(t_1(1,0), t_2(0,1), t_3(1,0), t_4(0,1), t_5(1,0), t_6(0,1)\right)$.

Table 8 Option prices in euros for different values of strike price K conditioning at each state and employing the density function obtained by considering the first six moments for $\mathbf{t}_0^6$ and strategy $\pi = \pi\left(t_1(1,0), t_2(0,1), t_3(1,0), t_4(0,1), t_5(1,0), t_6(0,1)\right)$.

K	$J_0 = 1$	$J_0 = 2$	$J_0 = 3$	$J_0 = 4$
1,500,000	121,767	454,730	904,717	1,209,253
2,000,000	6,626	24,017	35,534	91,908
2,500,000	5,146	6,387	1,039	1,294
3,000,000	5,141	6,289	1,024	1,213

Table 9 Option prices in euros for different values of strike price K conditioning at each state and employing the density function obtained by considering the lognormal distribution for $\mathbf{t}_0^6$ and strategy $\pi = \pi\left(t_1(1,0), t_2(0,1), t_3(1,0), t_4(0,1), t_5(1,0), t_6(0,1)\right)$.

K	$J_0 = 1$	$J_0 = 2$	$J_0 = 3$	$J_0 = 4$
1,500,000	109,877	563,202	862,124	941,136
2,000,000	5,426	45,842	52,279	134,620
2,500,000	4,080	4,953	5,873	6,014
3,000,000	3,561	3,666	3,032	3,024

By comparing the results in Tables 8 and 9, we observe that also, in this case, the B&S model exhibits a mispricing of the option in favor of the proposed model, confirming the results obtained in the previous subsection.

4 Conclusions

In this study, we show how to price an option that allow the airing of an advertisement on multiple television channels at certain times in exchange for a strike price. We model the number of viewers through a Markov chain, and we show how to compute the k-th moment of the total discounted cash flows through recurrent type equations. We apply the FGM copula to model the dependence structure existing between the dynamics of viewership of multiple channels. Indeed, we capture the degree of association in audience fluctuations and their joint impact on the total discounted cash flows. Finally, we use the method of moments with the maximum entropy approach by Mead and Papanicolaou (1984) to find the density function of the discounted cash flows and get the fair price of the option in dependence on different strike prices.

This work advances the methodology proposed in D'Amico et al (2024) by relaxing the assumptions of a single channel on which to air the advertisement and regular timetable for transmitting it. We introduce a modular strategy framework that gives the possibility of broadcasting the advertising at different times for each channel considered. Therefore, we overcome these limitations by proposing a more flexible strategy which allow for a more dynamic process, improving the effectiveness of advertising campaigns.

The analysis reveals that higher-order moments capture increasing deviations from the mean, particularly in higher states. This led to the observation that distributions conditioned on higher states tend to have heavier tails, emphasizing the likelihood of extreme events in viewership dynamics. We use the obtained density functions to compute option prices for different strike values. The results show that the option prices vary significantly across initial states, reflecting the different levels of uncertainty in expected revenues. The findings provide valuable insights into the financial implications of advertising strategies and demonstrate the relevance of moment-based density estimation in real option pricing.

From a policy perspective, this approach offers a rigorous quantitative framework to guide optimal allocation of advertising budgets across time slots and television networks. It supports broadcasters and advertisers in evaluating the value of flexible and modular strategies under uncertainty, encouraging more data-driven and cost-effective campaign planning. Additionally, regulators and stakeholders can use this model to assess the potential market impact of advertisement and the economic efficiency of scheduling policies in the broadcasting sector.

Future research could extend this approach by leveraging more detailed datasets to refine model accuracy and incorporate more sophisticated copulas. It could also be possible to consider additional stochastic factors affecting television viewership. Furthermore, applying this methodology to other industries with time-dependent revenue streams could enhance its applicability and robustness.

Author contributions All the authors contributed equally to this work. All authors read and approved the final manuscript.

Funding There is no source of funding to be reported.

Data availability Not applicable.

Declarations

Conflict of interest The authors declare that they have no Conflict of interest.

Ethical approval Not applicable.

Consent to participate Not applicable.

Consent for publication Not applicable.

References

Abdel Sabour, S.A., Poulin, R.: Valuing real capital investments using the least-squares monte carlo method. Eng. Econ. **51**(2), 141–160 (2006)

Abedi, V.S.: Allocation of advertising budget between multiple channels to support sales in multiple markets. J. Op. Res. Soc. **68**(2), 134–146 (2017)

Arslan, A., Tecimer, K., Turgut, H., et al.: A comprehensive framework for measuring the immediate impact of tv advertisements: Tv-impact. Entropy **26**(2), 109 (2024)

Auditel. Audience Measurement Data. https://www.auditel.it/en/data/, accessed: 2024-02-24 (2024)

Bharucha-Reid, A.: Statistical inference for markov processes (p billingsley). SIAM Rev. **4**(3), 262 (1962)

Billingsley, P.: Statistical methods in markov chains. Ann. Math. Stat. **35**, 12–40 (1961)

Black, F., Scholes, M.: The pricing of options and corporate liabilities. J. Political Econ. **81**(3), 637–654 (1973)

Cambanis, S.: Some properties and generalizations of multivariate eyraud-gumbel-morgenstern distributions. J. Multivar. Anal. **7**(4), 551–559 (1977)

Cherubini, U., Luciano, E., Vecchiato, W.: Copula Methods in Finance. John Wiley & Sons (2004)

Cox, J.C., Ross, S.A., Rubinstein, M.: Option pricing: a simplified approach. J. Financ Econ. **7**(3), 229–263 (1979)

Cucchiella, F., Gastaldi, M.: Risk management in supply chain: a real option approach. J. Manuf. Technol. Manag. **17**(6), 700–720 (2006)

D'Amico, G., Petroni, F., Prattico, F.: Wind speed prediction for wind farm applications by extreme value theory and copulas. J. Wind Eng. Indus. Aerodyn. **145**, 229–236 (2015)

Danaher, P.J., Rust, R.T.: Determining the optimal return on investment for an advertising campaign. Eur. J. Op. Res. **95**(3), 511–521 (1996)

Davis, R.M.: The role of the media in promoting and reducing tobacco use. 19, US Department of Health and Human Services, National Institutes of Health (2008)

Di Bari, A., Santoro, D., Tarrazon-Rodon, M.A., et al.: The impact of polarity score on real option valuation for multistage projects. Quality & Quantity **58**(1), 57–76 (2024)

Durante, F., Fernández-Sánchez, J., Quesada-Molina, J.J., et al.: Convergence results for patchwork copulas. Eur. J. Op. Res. **247**(2), 525–531 (2015)

D'Amico, G., Petroni, F., Regnault, P., et al.: A copula-based markov reward approach to the credit spread in the european union. Appl. Math. Finance **26**(4), 359–386 (2019)

D'Amico, G., Masala, G., Petroni, F., et al.: Managing wind power generation via indexed semi-markov model and copula. Energies **13**(16), 4246 (2020)

D'Amico, G., De Blasis, R., Vigna, V.: Advertising investments on television: real option estimation through markov chains. Quality & Quantity **58**(5), 4661–4678 (2024)

Gabriel, B.J., Leonardo, M., Miriam, S.: Modeling multivariate tourism expenditure using vine copula: empirical findings from of fribourg-switzerland. Quality & Quantity **58**(5), 4093–4116 (2024)

Goodwin, B.K., Rivieccio, G., De Luca, G., et al.: Computing impulse response functions from a copula-based vector autoregressive model: evidence from the italian agri-food value chain. Quality & Quantity **58**(2), 1779–1797 (2024)

Hu, W., Min, Y., Zhou, Y., et al.: Wind power forecasting errors modelling approach considering temporal and spatial dependence. J. Modern Power Syst. Clean Energy **5**, 489–498 (2017)

Joshi, A., Hanssens, D.M.: The direct and indirect effects of advertising spending on firm value. J. Market. **74**(1), 20–33 (2010)

Krishnamurthi, L., Raj, S.P.: The effect of advertising on consumer price sensitivity. J. Market. Res. **22**(2), 119–129 (1985)
Lo, K.H., Lan, Y.W.: An approach to the r &d value based upon real option method. Quality & Quantity **44**, 509–527 (2010)
Martín-Oliver, A., Salas-Fumás, V.: The output and profit contribution of information technology and advertising investments in banks. J. Financ. Int. **17**(2), 229–255 (2008)
Mead, L.R., Papanicolaou, N.: Maximum entropy in the problem of moments. J. Math. Phys. **25**(8), 2404–2417 (1984)
Oetzel, S., Luppold, A.: Is advertising overrated? return on marketing investment. In: 33 Phenomena of Purchasing Decisions: Understanding Customer Behavior-Knowledge and Inspiration. Springer, p 135–139 (2024)
O'Keefe, G.J., Reid, .K: The uses and effects of public service advertising. In: Public relations research annual. Routledge, p 67–92 (2020)
Papaefthymiou, G., Kurowicka, D.: Using copulas for modeling stochastic dependence in power system uncertainty analysis. IEEE Trans. Power Syst. **24**(1), 40–49 (2008)
Pauzé, E., Potvin Kent, M.: Children's measured exposure to food and beverage advertising on television in toronto (canada), May 2011-may 2019. Can. J. Public Health **112**(6), 1008–1019 (2021)
Pechmann, C., Catlin, J.R.: The effects of advertising and other marketing communications on health-related consumer behaviors. Curr. Opin. Psychol **10**, 44–49 (2016)
Tellis, G.J., Chandy, R.K., MacInnis, D., et al: Modeling the microeffects of television advertising: Which ad works, when, where, for how long, and why? Marketing Science pp 359–366 (2005)